Effects of Induction Interactions on the Orientational Order of Solutes in Liquid Crystals

Andrea di Matteo† and Alberta Ferrarini*

Dipartimento di Chimica Fisica, Università di Padova, 2 via Loredan, 35131 Padova, Italy

Received: November 7, 2000; In Final Form: January 25, 2001

In a recent paper (di Matteo, A.; Ferrarini, A.; Moro, G. J. *J. Phys. Chem. B* **2000**, *104*, 7764) a method to derive a mean field potential for molecules in nematic phases based on their structure and charge distribution has been presented. The potential consists of a shape and a reaction field contribution, accounting for short range and electrostatic intermolecular interactions, respectively. The model is extended here by introducing induction interactions in the reaction field. In the spirit of our approach, aimed at a realistic picture at a semiphenomenological level, an appropriate description is obtained in terms of distributed polarizabilities. The Thole model of interacting damped atom dipoles has been singled out as a suitable one, although also different choices have been considered. The orientational order parameters calculated in this way for a set of typical polar and nonpolar solutes in nematic solvents are reported, and the influence of induction interactions is discussed.

I. Introduction

Electrostatic interactions between molecules play a relevant role in determining the properties of condensed phases. They affect, to a greater or lesser extent, phase transitions and solvation processes and can produce significant changes in the response of single molecules to electric fields, besides, of course, determining the macroscopic dielectric behavior. It is then clear the importance of developing methods to handle electrostatic interactions, not only from the fundamental point of view of gaining insights into the properties of condensed phases, but also with the application purpose of predicting material behavior. This is not an easy task, because both suitable descriptions of the electric properties of molecules and appropriate methods to treat many-body interactions are required. Actually, the importance of the problem was early recognized and much work has been done in different directions. On one side sophisticated quantum mechanical approaches have been developed for the evaluation of molecular electric properties; in this framework also interactions with the surroundings can be included in the molecular Hamiltonian in terms of reaction field (for recent reviews see refs 1−3). On the other hand, the description of condensed phase systems can be achieved by Monte Carlo or molecular dynamics simulations, and methods to deal with the long-range electrostatic interactions have been set up (a vast literature on this subject is available; refs 4−6 are only given as examples). Classical intermolecular potentials are adopted, which, however, can be constructed on the basis of molecular properties; detailed potentials can be used, at the expense of the computational requirements.[7] It is also possible, at least for simple systems, to perform fully ab initio simulations, but with a much higher CPU demand.[8] Therefore, it is important to devise, in parallel with the aforementioned methods, alternative procedures which, by combining a detailed account of the relevant molecular features and an approximate treatment of intermolecular interactions, allow the evaluation of condensed phase properties even for systems of a certain complexity.[9−13]

A typical case is that of liquid crystal phases, which are composed of relatively large and flexible molecules carrying nonnegligible electric dipoles.[14] The formation of mesophases can be related to their elongated shape. In other words, excluded volume and short-range attractions, which are modulated by the molecular shape, are recognized to have the main responsibility for the onset of orientational order. Thus, in all generality it can be stated that orientational order is promoted by an increase of the molecular anisometry. On the contrary, there is no clear evidence of the role played by electrostatic interactions. These are expected to have some relevance; however, little is known not only about their magnitude but also about their qualitative influence.[15,16] The effects of the presence of dipoles on mesophase properties have been investigated by computer simulations on systems of ellipsoids or spherocylinders interacting with simplified potentials,[17,18] and the dependence upon magnitude and location of the dipoles has been determined. A more realistic account of molecular features was included in a statistical-mechanical approach, based on a cluster expansion method;[19] in this way the authors could predict the orientational order of simple rigid solutes, described in terms of their shape, electric dipole, and quadrupole moments and polarizability, in nematic solvents approximated as spherocylinders characterized by their aspect ratio and dipole moment. In a recent work[20] a mean-field method combining a shape model for short-range anisotropic interactions, the so-called surface tensor model,[21] and the reaction field approximation for electrostatic interactions[22] was presented. The reaction field was calculated by exploiting a mathematical treatment that allows the reformulation of the electrostatic problem in terms of integral equations on the molecular surface, even in the case of anisotropic phases.[23] Within our approach the properties of the probe molecule, in this case the morphology of its surface and its charge distribution, which is described in terms of point charges at the nuclear positions, are accounted for in detail, while the medium is viewed as a continuum, characterized by its orienting strength and dielectric permittivity. The model was applied for the prediction of orientational order parameters of simple rigid solutes, polar and nonpolar, in nematic solvents. In this way it

* Corresponding author. E-mail: a.ferrarini@chfi.unipd.it.
† E-mail: a.dmatteo@chfi.unipd.it.

10.1021/jp0040805 CCC: $20.00
Published on Web 03/21/2001

was possible to correlate with the dielectric anisotropy of the solvent the change of order observed for a given molecule when dissolved in different solvents. The theoretical predictions were in qualitative agreement with experimental data, although in all cases electrostatic effects appeared to be underestimated. One of the possible reasons for such a behavior could be the neglect of induction interactions. In our model the molecular charge distribution was identified with a set of atomic charges calculated for the isolated molecule; however, it is reasonable to expect that the charge distribution of a molecule can be significantly influenced by its environment. From simple estimates based on the Onsager model, the effective dipole moment of polar molecules in the liquid phase is expected to be from 20 to 50% larger than in the gas phase.[22] Indeed, there is general consensus about the importance of induction effects in determining condensed phase properties, and in modern computational techniques methods to account for them keep being developed.[9,11,12,24,25] In our case the perspective is somehow peculiar, since effects on orientational order depend not just upon the magnitude of induction interactions but rather upon their orientation dependence. The following mechanism can be envisaged: the molecular charge distribution polarizes the surrounding dielectric; this reaction field in turn polarizes the electronic cloud of the probe molecule and, in response to the induced charges in the molecule, the solvent polarization increases. Simple arguments, based on the consideration that the charge distribution induced in the molecule by the environment polarization should reflect the permanent charge distribution, lead us to expect that induction interactions should enhance the anisotropy of the electrostatic contribution to orientational order. This is certainly true for a polarizable dipole in a spherical cavity;[22] for more complex charge distributions and cavity shapes, it has to be proven by calculations. To investigate this aspect, we have generalized the reaction field model presented in ref 20 by introducing, in addition to permanent charges, an induced charge distribution described in terms of polarizability.

The essentially additive contribution of the different groups in a molecule to the overall polarizability has been recognized, and much effort has been devoted to the development of reasonable additive schemes, with the identification of the elementary transferable contributions and their parametrization. Several models have been presented, with parametrizations derived from theoretical analyses or simply from fits of experimental or ab initio molecular polarizabilities.[26−34] The lowest level approximation is based on the assumption of noninteracting isotropic atom dipoles and can only be used for the prediction of the isotropic part of the polarizability tensor. More complex methods involve distributions of interacting multipoles; as a consequence of the mutual couplings, even in their simplest form of isotropic atomic contributions they are able to account for the anisotropy deriving from the molecular geometry. More recently, the so-called fluctuating charge and chemical potential equalization methods have been proposed, based on the principle of electronegativity equalization in the system.[35,36] The choice of the approach to be used is related to the problem under investigation. In our case the model is required to be able to map in a reliable way the response of the electronic density to a nonuniform field, as the reaction field is, with a sufficiently accurate account of the anisotropy of such a response. Moreover, the model should possibly meet the requirements of general applicability and computational handiness, to allow the use for different classes of molecules and to avoid increasing too much the heaviness of the already demanding reaction field calculations.[20] An appropriate choice has been envisaged in the Thole model of damped atomic interacting dipoles,[33] which has the advantages of being simple and of fairly general use, having been parametrized over a wide set of molecules.[37,38] Such a model has been used also for molecular dynamics simulations,[39] molecular mechamics force fields,[40] and reaction field calculations.[41]

The paper is organized in the following way. In the next section the generalization of the reaction field treatment including polarization effects will be presented, with particular reference to the Thole model for polarizability. In section III the features of the orienting mean field potential for molecules in nematic phases, with a surface tensor and a reaction field contribution, are outlined; a more thorough discussion is reported in ref 20. Section IV summarizes the main points of the computational procedure, while in section V the results obtained for a set of test solutes in nematic solvents will be presented and discussed. Conclusive remarks are given in section VI.

II. Reaction Field

The electrostatic potential $V(\vec{r})$ deriving from a charge distribution $\rho(\vec{r})$ contained in a cavity C embedded in a dielectric with permittivity ϵ is the solution of the differential equations

$$\begin{aligned} -(\partial/\partial\vec{r})\cdot\epsilon\cdot(\partial/\partial\vec{r})V(\vec{r}) &= 0 \qquad \text{outside } C \\ -\partial^2/\partial\vec{r}^{\,2}\, V(\vec{r}) &= \rho(\vec{r})/\epsilon_0 \qquad \text{inside } C \end{aligned} \tag{1}$$

with the boundary conditions on the surface S of the cavity:

$$\begin{aligned} V_e(\vec{r}) - V_i(\vec{r}) &= 0 \qquad \text{on } S \\ [\partial V(\vec{r})/\partial\vec{r}]_i\cdot\hat{s}(\vec{r}) - \epsilon[\partial V(\vec{r})/\partial\vec{r}]_e\cdot\hat{s}(\vec{r}) &= 0 \qquad \text{on } S \end{aligned} \tag{2}$$

where $\hat{s} = \hat{s}(\vec{r})$ is the normal outward pointing unit vector in $\vec{r}$, and the subscripts e and i denote the values on the surface of functions defined inside and outside the cavity. The electrostatic potential $V(\vec{r})$ is the superposition of the potential generated by the charge distribution $\rho(\vec{r})$ in a vacuum, hereafter denoted as $\varphi(\vec{r})$, and a contribution deriving from the polarization of the surrounding dielectric, which depends on the charge distribution inside the cavity, on the permittivity ϵ and on the cavity shape (reaction field). According to the integral equation formalism presented in ref 23 and used in ref 20 to calculate the electrostatic contribution to the orienting mean field potential in the nematic phase, the reaction field effects can be expressed in terms of an apparent charge density distributed over the molecular surface, $\sigma(\vec{r},\omega)$, which in anisotropic phases (with anisotropic dielectric permittivity) depends on the molecular orientation ω. This is the solution of the integral equation

$$A\sigma = -g \tag{3}$$

with

$$A = \left(\frac{I}{2} - D_e\right)S_i + S_e\left(\frac{I}{2} + D_i\right) \tag{4}$$

and

$$g = \left(\frac{I}{2} - D_e\right)\varphi - S_e\epsilon_0 E_n \tag{5}$$

In these equations $E_n = -\hat{s}\cdot(\partial/\partial\vec{r})\varphi(\vec{r})$ is the normal to the surface component of the electric field in a vacuum, while S_i, D_i, S_e, and D_e are integral operators on the space of functions

$u(\vec{r})$ defined on the surface ($\vec{r} \in S$) and I is the identity operator

$$(S_i u)(\vec{r}) = \int_S G_i(\vec{r},\vec{r}')\, u(\vec{r}')\, d\vec{r}'$$

$$(D_i u)(\vec{r}) = \int_S u(\vec{r}')\, \hat{s}(\vec{r}) \cdot \left[\epsilon_0 \frac{\partial}{\partial \vec{r}} G_i(\vec{r}, \vec{r}')\right] d\vec{r}'$$

$$(S_e u)(\vec{r}) = \int_S G_e(\vec{r},\vec{r}')\, u(\vec{r}')\, d\vec{r}'$$

$$(D_e u)(\vec{r}) = \int_S u(\vec{r}')\, \hat{s}(\vec{r}') \cdot \left[\epsilon_0 \epsilon \frac{\partial}{\partial \vec{r}'} G_e(\vec{r},\vec{r}')\right] d\vec{r}' \quad (6)$$

which employ the Green functions for the electrostatic problem inside and outside the cavity

$$G_i(\vec{r},\vec{r}') = \frac{1}{4\pi\epsilon_0 |\vec{r} - \vec{r}'|}$$

$$G_e(\vec{r},\vec{r}') = \frac{1}{4\pi\epsilon_0 \sqrt{\det(\epsilon)(\vec{r} - \vec{r}') \cdot \epsilon^{-1} \cdot (\vec{r} - \vec{r}')}} \quad (7)$$

Under the assumption that the molecular charge distribution is not affected by the interaction with the environment (nonpolarizable molecules), considered in ref 20, the electrostatic potential and field appearing in eq 5 are simply due to the permanent charge distribution $\rho^0(\vec{r})$ contained in the cavity; so, using the zero apex to refer to permanent charges, we can write

$$g = g^0 = \left[\left(\frac{I}{2} - D_e\right) + \epsilon_0 S_e \hat{s} \cdot \frac{\partial}{\partial \vec{r}}\right] \varphi^0(\vec{r}) \quad (8)$$

In the case of N charges located at the nuclear positions the potential $\varphi^0(\vec{r})$ is given by

$$\varphi^0(\vec{r}) = \frac{1}{4\pi\epsilon_0} \sum_{J=1}^{N} \frac{\rho_J^0}{|\vec{r} - \vec{r}_J|} \quad (9)$$

where $\rho_J^0 = \rho^0(\vec{r}_J)$. A more realistic description should take into account the fact that the molecular charge distribution is modified by an applied electric field, as is the reaction field in our case. This can be done by considering, besides the electrostatic potential φ^0 and field $\vec{E}^0$, additional terms accounting for the deformation of the electron cloud in the molecule:

$$\varphi(\vec{r}) = \varphi^0(\vec{r}) + \varphi^{ind}(\vec{r})$$
$$\vec{E}(\vec{r}) = \vec{E}^0(\vec{r}) + \vec{E}^{ind}(\vec{r}) \quad (10)$$

where the apex "ind" is used for the contributions induced by the applied field.

Molecular Polarizability. A convenient way to take into account the response of the electron cloud to the reaction field, in the spirit of our approach and in agreement with the additive nature of polarizability, consists of assuming a superposition of contributions deriving from all atoms. Although, in all generality, a multipole expansion of the induced charge distribution should be performed,[32,42] usually only the dipolar term is retained; thus the induced dipole at the Jth atomic position can be expressed as

$$\vec{\mu}_J^{ind} = \boldsymbol{\alpha}_J \vec{E}_J \quad (11)$$

where $\boldsymbol{\alpha}_J$ is the atomic polarizability tensor of the Jth atom and $\vec{E}_J$ is the local electric field at its center.

At the lowest level of approximation, independent contributions from each atom are considered, and the response of the whole molecule is accounted for by a polarizability that is the sum of atomic terms, $\alpha = \sum_{J=1}^{N} \boldsymbol{\alpha}_J$. If, in addition, the atomic polarizabilities are assumed to be isotropic, i.e., $\boldsymbol{\alpha}_J = \alpha_J \mathbf{I}_3$ where $\mathbf{I}_3$ is a 3×3 unit matrix, also the molecular polarizability results to be isotropic. This approximation which, although rather unrealistic, might be used in considering properties determined by the average polarizability, appears to be too crude when a dependence on the anisotropy of the polarizability cannot be excluded. A more realistic description can be achieved by the so-called interaction models, which take into account the mutual couplings between the induced dipoles. In this case the local field $\vec{E}_J$ in eq 11 is determined by both the reaction field and the fields due to all the other induced dipoles (mutual induction); the induced dipole at the Jth atom is then given by

$$\vec{\mu}_J^{ind} = \boldsymbol{\alpha}_J (\vec{R}_J - \sum_{I \neq J} \mathbf{T}_{JI} \vec{\mu}_I^{ind}) \quad (12)$$

where $\vec{R}_J$ is the reaction field at the Jth position, and $\mathbf{T}_{JI} = \mathbf{T}_I(\vec{r}_J)$ is the interaction or dipole field tensor, expressing the field at the Jth nuclear position due to the presence of a dipole on the Ith atom. The tensor $\mathbf{T}_I(\vec{r})$ is defined as

$$\mathbf{T}_I(\vec{r}) = \frac{\mathbf{I}_3}{4\pi\epsilon_0 |\vec{r} - \vec{r}_I|^3} - \frac{3(\vec{r} - \vec{r}_I) \otimes (\vec{r} - \vec{r}_I)}{4\pi\epsilon_0 |\vec{r} - \vec{r}_I|^5} \quad (13)$$

where $\mathbf{I}_3$ is a 3×3 unit tensor.

Equation 12 can be rearranged into the single matrix equation

$$\mathbf{M}\, \boldsymbol{\mu}^{ind} = \mathbf{R} \quad (14)$$

where $\boldsymbol{\mu}^{ind}$ and $\mathbf{R}$ are column supermatrices of dimension $3N$ having as elements the Cartesian components of the vectors $\vec{\mu}_J^{ind}$ and $\vec{R}_J$ and $\mathbf{M}$ is a $3N \times 3N$ supermatrix; they are defined as

$$\mathbf{M} = \begin{bmatrix} \boldsymbol{\alpha}_1^{-1} & \boldsymbol{T}_{12} & \dots & \mathbf{T}_{1N} \\ \mathbf{T}_{21} & \boldsymbol{\alpha}_2^{-1} & \mathbf{T}_{2N} & \\ \vdots & \vdots & \vdots & \\ \mathbf{T}_{N1} & \mathbf{T}_{N2} & \dots & \boldsymbol{\alpha}_N^{-1} \end{bmatrix} \quad \boldsymbol{\mu}^{ind} = \begin{bmatrix} \vec{\mu}_1^{ind} \\ \vec{\mu}_2^{ind} \\ \vdots \\ \vec{\mu}_N^{ind} \end{bmatrix} \quad \mathbf{R} = \begin{bmatrix} \vec{R}_1 \\ \vec{R}_2 \\ \vdots \\ \vec{R}_N \end{bmatrix} \quad (15)$$

Then, the dipole moments $\vec{\mu}_J^{ind}$ can be obtained by matrix inversion as

$$\mu_{J\eta}^{ind} = \sum_{I=1}^{N} \sum_{\zeta} [\mathbf{M}^{-1}]_{J\eta I\zeta} R_{I\zeta} \qquad \text{with} \qquad \eta,\zeta \in \{x, y, z\} \quad (16)$$

It appears from this equation that the supermatrix $\mathbf{M}^{-1}$, usually denoted as relay matrix, gives an atomic representation of the polarizability. The molecular polarizability can be obtained by contraction of this matrix

$$\alpha_{\eta\zeta}^{mol} = \sum_{I=1}^{N} \sum_{J=1}^{N} [\mathbf{M}^{-1}]_{J\eta I\zeta} \quad (17)$$

The dipole field tensors eq 13 carry in the dependence on the geometry of the molecular arrangement. Therefore, anisotropic molecular polarizabilities are obtained in this way, with the same symmetry of the molecular structures, even though isotropic atom polarizabilities are assumed.

It can be easily shown that this model provides unrealistic predictions in the presence of an electric field parallel to the line joining two nearby dipoles, as occurs for a field parallel to

the long axis of a diatomic molecule. In this case if two atoms are closer than a given distance, which depends on their polarizabilities, the head-to-tail interaction between them causes the molecular polarizability to diverge to infinity. This problem can be avoided by damping the interactions between dipoles close to each other. A modified dipole tensor including a distance-dependent attenuation has been proposed by Thole.[33] The underlying idea is that induced dipoles are smeared out around nuclei, so that a given polarizable center feels only part of the charge distribution centered on another atom if this lies too close. By assuming a linear dependence on distance of the charge density, he obtained the following form for the dipole tensor

$$\mathbf{T}_{IJ} = \mathbf{T}_I(\vec{r}_J) = \frac{4v_{IJ}^3 - 3v_{IJ}^4}{4\pi\epsilon_0|\vec{r}_J - \vec{r}_I|^3}\boldsymbol{I}_3 - \frac{3v_{IJ}^4(\vec{r}_J - \vec{r}_I)\otimes(\vec{r}_J - \vec{r}_I)}{4\pi\epsilon_0|\vec{r}_J - \vec{r}_I|^5} \quad (18)$$

with

$$v_{IJ} = \begin{cases} r_{IJ}/s_{IJ} & \text{for } r_{IJ} < s_{IJ} \\ 1 & \text{for } r_{IJ} \geq s_{IJ} \end{cases} \quad (19)$$

where s_{IJ} is a scaling distance. Thus, if atoms I and J are farther away than the scaling distance, eq 13 is recovered. In the original formulation the scaling distance is defined as[33]

$$s_{IJ} = x(\alpha_I\alpha_J)^{1/6} \quad (20)$$

where $\alpha_{I(J)}$ is the atom isotropic polarizability and x is a parameter related to the width of the charge density distribution, which can be used as a fitting parameter in comparing theoretical and experimental (or ab initio) polarizabilities.[37] Also, alternative definitions of the scaling parameters, and then different parametrizations, have recently been proposed.[38]

In the original formulation and in subsequent revisions of the Thole model isotropic atomic polarizabilities are assumed. This seems to be rather unrealistic in the case of molecules with π-electron systems, which are characterized by a very anisotropic polarizability, with a more pronounced deformability in the plane of the π distribution. An appropriate model of polarizability was proposed for these systems, which is a modification of the atom dipole approach, with the introduction of different atomic polarizabilities in plane and out of plane for the π system and of a further contribution of charge transfer among atoms.[30,32] The inclusion of new details is made at the cost of increasing the number of parameters of the model and its computational complexity. The main points of the model are sketched in the Appendix.

Induction Effects in the Reaction Field Model. Electric field and potential generated at the point $\vec{r}$ by the induced dipoles can be written by summing the effect of all induced dipoles contained in the cavity

$$\varphi^{\text{ind}}(\vec{r}) = \sum_{J=1}^{N}\vec{t}_J(\vec{r})\cdot\vec{\mu}_J^{\text{ind}}$$

$$\vec{E}^{\text{ind}}(\vec{r}) = -\sum_{J=1}^{N}\mathbf{T}_J(\vec{r})\cdot\vec{\mu}_J^{\text{ind}} \quad (21)$$

with the dipole tensor $\mathbf{T}_J(\vec{r})$ defined in eq 13 and the vector $\vec{t}_J(\vec{r})$ defined as

$$\vec{t}_J(\vec{r}) = \frac{\vec{r} - \vec{r}_J}{4\pi\epsilon_0|\vec{r} - \vec{r}_J|^3} \quad (22)$$

Now, by substituting the expressions for the induced dipole moments, eq 14, and recalling that the reaction field can be evaluated from the apparent charge density σ on the molecular surface as

$$\vec{R}_I = \frac{1}{4\pi\epsilon_0}\int_S \frac{\vec{r}_I - \vec{r}}{|\vec{r}_I - \vec{r}|^3}\sigma(\vec{r})\,\mathrm{d}\vec{r} = -\int_S\vec{t}_I(\vec{r})\,\sigma(\vec{r})\,\mathrm{d}\vec{r} \quad (23)$$

the following expressions are obtained for the electrostatic potential and field arising from the induced dipoles:

$$\varphi^{\text{ind}}(\vec{r}) = -\sum_{I,J}\vec{t}_J(\vec{r})\cdot[\mathbf{M}^{-1}]_{JI}\cdot\int_S\vec{t}_I(\vec{r}')\,\sigma(\vec{r}')\,\mathrm{d}\vec{r}'$$

$$\vec{E}^{\text{ind}}(\vec{r}) = \sum_{I,J}\mathbf{T}_J(\vec{r})\cdot[\mathbf{M}^{-1}]_{JI}\cdot\int_S\vec{t}_I(\vec{r}')\,\sigma(\vec{r}')\,\mathrm{d}\vec{r}' \quad (24)$$

where $[\mathbf{M}^{-1}]_{JI}$ is the 3×3 block of the relay matrix corresponding to Ith and Jth atoms and the dot indicates contraction over Cartesian coordinates. Much simpler expressions would result if the additive model were considered, in which case $[\mathbf{M}^{-1}]_{JI} = \alpha_J\delta_{IJ}\mathbf{I}_3$.

The apparent charge density σ on the surface of a cavity containing a set of permanent and induced charges can now be calculated by solving the integral equation

$$A\,\sigma = -g^0 - g^{\text{ind}} \quad (25)$$

where g^0 is given by eq 8, while

$$g^{\text{ind}} = \left(\frac{I}{2} - D_e\right)\varphi^{\text{ind}} - \epsilon_0 S_e E_n^{\text{ind}} \quad (26)$$

Since the potential and field arising from induced dipoles, eq 24, have a linear dependence on the apparent charge density σ, the latter expression can be rewritten as $g^{\text{ind}} = A^{\text{ind}}\sigma$, with the linear operator A^{ind} defined by

$$(A^{\text{ind}}\sigma)(\vec{r}) = \sum_{I,J}\left\{-\left(\frac{I}{2} - D_e\right)\vec{t}_J(\vec{r})\cdot[\mathbf{M}^{-1}]_{JI} - \epsilon_0 S_e\hat{s}\cdot\mathbf{T}_J(\vec{r})\cdot[\mathbf{M}^{-1}]_{JI}\right\}\cdot\int_S\vec{t}_I(\vec{r}')\,\sigma(\vec{r}')\,\mathrm{d}\vec{r}' \quad (27)$$

Thus, the introduction of induced charges leads to a new integral equation which differs from that derived in the case of permanent charges for the presence of an additional linear contribution:

$$(A + A^{\text{ind}})\sigma = -g^0 \quad (28)$$

A being the operator defined in eq 4.

On the basis of the charge density σ, which is the solution of the integral eq 28, it is possible to calculate all reaction field properties; in particular we shall consider, the energy of the polarizable charge distribution $\rho^0(\vec{r})$ in its reaction field:[22]

$$U_{\text{rf}}(\omega) = \frac{1}{2}\int_S\varphi^0(\vec{r})\,\sigma(\vec{r})\,\mathrm{d}\vec{r} \quad (29)$$

and the atomic dipoles induced in the molecule, which by

substituting eq 23 in eq 16 are given by

$$\mu_{J\eta}^{\mathrm{ind}} = -\sum_{I=1}^{N}\sum_{\zeta}\mathbf{M}_{J\eta I\zeta}^{-1}\int_S t_{I\zeta}(\vec{r})\,\sigma(\vec{r})\,\mathrm{d}\vec{r} \qquad \text{with}$$

$$\eta,\zeta \in \{x, y, z\} \quad (30)$$

We can recall that an alternative procedure for the calculation of the apparent surface charge density σ could be devised in the iterative solution of the set of coupled equations in the unknown σ and $\boldsymbol{\mu}^{\mathrm{ind}}$

$$\begin{cases} A\,\sigma = -g^0 - g^{\mathrm{ind}} \\ \boldsymbol{M}\boldsymbol{\mu}^{\mathrm{ind}} = \boldsymbol{R} \end{cases} \quad (31)$$

with g^{ind}, $\boldsymbol{\mu}^{\mathrm{ind}}$, and **R** defined according to eqs 26, 16, and 23, respectively, the electrostatic potential and field being derived from the induced dipoles according to eqs 24. In this way no inversion of the matrix **M** would be required. However, it can be seen that for molecular dimensions lower than a few hundreds of atoms the advantage of avoiding the matrix inversion does not compensate the cost of repeatedly solving the linear system eqs 31.

III. Mean Field Potential

The orienting mean field potential experienced by a molecule in the liquid crystal phase is written as the sum of a surface tensor contribution, U_{st}, accounting for short-range interactions, and a reaction field term, U_{rf}, describing electrostatic interactions:[20]

$$U(\omega) = U_{\mathrm{st}}(\omega) + U_{\mathrm{rf}}(\omega) \quad (32)$$

where the dependence upon the director orientation in the molecular frame, specified by the polar angles $\omega = (\theta,\phi)$, is indicated.

The surface tensor contribution[21,43] is derived on the basis of the consideration that the anisotropy of short-range interactions is determined by the anisometry of the molecular shape; in particular, by exploiting the analogy with the anchoring free energy of macroscopic surfaces, it is assumed that each (infinitesimal) surface element dS of a molecule tends to orient its normal $\hat{s}$ perpendicular to the director $\hat{n}$ of the mesophase. Such a behavior is accounted for by an energy contribution which, after truncating at the first nonisotropic and nonpolar term the expansion with respect to $\hat{n}\cdot\hat{s}$, is written as $\mathrm{d}U_{\mathrm{st}} = \xi P_2(\hat{n}\cdot\hat{s})\,\mathrm{d}S$, where P_2 is the second Legendre polynomial and ξ [44] is the temperature-dependent strength of the interaction. The overall potential acting on a molecule is derived by integrating these elementary contributions over the whole molecular surface

$$U_{\mathrm{st}}(\omega) = \xi\int_S P_2(\hat{n}\cdot\hat{s})\,\mathrm{d}\vec{r} \quad (33)$$

its orientational dependence can be made explicit by using the addition theorem for spherical harmonics:[45]

$$U_{\mathrm{st}}(\omega) = -\xi\sum_m T^{2,m} * C_{2m}(\omega) \quad (34)$$

where $C_{Lm}(\omega) = \sqrt{4\pi/(2L+1)}\,Y_{Lm}(\omega)$ are modified spherical harmonics,[45] and $T^{2,m}$ are irreducible spherical components of a traceless second rank tensor denoted as the surface tensor

$$T^{2,m} = -\int_S C_{2m}(\theta_s,\phi_s)\,\mathrm{d}\vec{r} \quad (35)$$

with the polar angles (θ_s, ϕ_s) identifying the orientation, in the molecular frame, of the normal $\hat{s}$ to the surface element dS. It follows from the definition that the diagonal Cartesian component T_{ii} of the surface tensor is related to the anisometry of the molecular surface perpendicular to the ith molecular axis. A high positive (negative) value of T_{ii} indicates a strong tendency of the molecule to align the ith axis parallel (perpendicular) to the mesophase director.

The reaction field contribution to the mean field potential eq 32 corresponds to the free energy of the charge distribution contained in the cavity embedded in the dielectric, which is equal to the work spent to produce the same charge distribution and is given by eq 29.[22] Again, the angular dependence of the reaction field potential is conveniently represented in terms of modified spherical harmonics

$$U_{\mathrm{rf}}(\omega) = \sum_{L(\mathrm{even})}\sum_m F^{L,m} * C_{L,m}(\omega) \quad (36)$$

where the sum is restricted to even values of the rank L in view of the phase symmetry, and the coefficients $F^{L,m}$ are defined as

$$F^{L,m} = \frac{2L+1}{4\pi}\int U_{\mathrm{rf}}(\omega)C_{Lm}^{*}(\omega)\,\mathrm{d}\omega \quad (37)$$

The orientational behavior of a molecule in the liquid crystal phase is described by the distribution function $f(\omega)$, which is related to the mean field potential $U(\omega)$

$$f(\omega) = \frac{\exp[-U(\omega)/k_{\mathrm{B}}T]}{\int \exp[-U(\omega)/k_{\mathrm{B}}T]\,\mathrm{d}\omega} \quad (38)$$

Actually, it is common to characterize the orientational behavior in terms of the Saupe ordering matrix:[14]

$$S_{ij} = \frac{1}{2}\int(3n_in_j - \delta_{ij})f(\omega)\,\mathrm{d}\omega \quad (39)$$

n_i being the projection of the unit vector $\hat{n}$ on the ith molecular axis. This is a symmetric traceless matrix; therefore in its principal frame there are only two independent elements, usually chosen as S_{ii}, measuring the degree of alignment of the ith principal axis, and $S_{jj} - S_{kk}$, which gives the biaxiality of ordering perpendicular to the ith axis.

Parametrization of the Mean Field Potential. Both surface and reaction field contributions to the mean field potential, eq 32, depend on structural characteristics of the probe molecule, i.e., molecular surface, atomic charges, and polarizabilities, which are accounted for in a detailed way, as explained above. In addition, there are solvent properties, i.e., the orienting strength ξ and the permittivity ϵ, whose values determine the weights of the two contributions to the mean field potential and their temperature dependence. For the sake of simplicity, in the spirit of the Maier−Saupe model,[14] these are assumed to be proportional to the solvent order parameter $\bar{P}_2^{s}$, which in turn only depends on the reduced temperature $T^* = T/T^{NI}$. The following expressions have been assumed:

$$\Delta\epsilon = \Delta\epsilon^{NI}\bar{P}_2^{\,s}/\bar{P}_2^{\,s,NI} \quad (40)$$

and

$$\xi = \xi_0 \bar{P}_2^{\,s} T^{NI} / T_s^{\,20} \tag{41}$$

with the index *NI* denoting transition values, T_s^{20} being the only nonzero component of the surface tensor of the solvent molecules, assumed to be axially symmetric.[21] The form of the orienting strength parameter is derived from the comparison of the surface tensor potential for solvent molecules, taken as rigid uniaxial objects, $U_s = -\xi T_s^{20} P_2(\cos\vartheta)$, and the Maier−Saupe expression $U_s = -\xi_0(\bar{P}_2^{\,s} T^{NI}) P^2(\cos\vartheta)$, where ξ_0 is universal constant.

IV. Computational Methods

The computational procedure followed for the calculation of order parameters is outlined in detail in ref 20, therefore only the main points will be summarized here, pointing out the differences due to the introduction of polarizability.

The electrostatic problem is solved according to the boundary element method; in this way the integral equation 28 is transformed into a set of algebraic equations by discretization over a grid of N^T tesserae on the molecular surface. The observables of interest are then calculated as

$$o = \boldsymbol{v}^T \mathbf{A}'^{-1} \mathbf{g}^0 \tag{42}$$

where $\mathbf{A}'$ and $\mathbf{g}^0$ are respectively the matrix and vector representing the operator $A' = A + A^{\,\mathrm{ind}}$, eqs 4 and 27, and the function g^0, eq 8. The explicit form of the elements of the matrices corresponding to the integral operators appearing in the expressions of A' and g^0 are reported in ref 20. The form of the vector $\boldsymbol{v}$ depends on the observable to be calculated. So, in the case of the reaction field contribution to the mean field potential, eq 29, its components are given by the values of electrostatic potential φ^0 at the surface tesserae

$$v_k = -a_k \varphi^0(\vec{r}_k)/2 \tag{43}$$

where a_k is the surface area of the kth tessera; for the evaluation of the η Cartesian component of the induced dipole at the Jth atom position, eq 30, the elements of $\mathbf{v}$ are given by

$$v_k = a_k \mu_{J\eta}^{\mathrm{ind}} = a_k \sum_{I=1}^{N} \sum_{\zeta} \mathbf{M}^{-1}_{J\eta I\zeta} t_{I\zeta}(\vec{r}_k) \text{ with } \eta,\zeta \in \{x, y, z\} \tag{44}$$

The inclusion of induction interactions introduces the additional term $\mathbf{A}^{\mathrm{ind}}$ in the $\mathbf{A}'$ matrix, defined according to eq 27. Its evaluation requires a series of matrix products and the inversion of the $\mathbf{M}$ matrix; matrices are of dimension $3N$, N being the number of atoms. The Gauss−Jordan algorithm is used for matrix inversion, which can be done at relatively low computational cost for molecules with a number of of atoms $N \leq 100$.

Equation 42 is solved with the biconjugate gradient algorithm;[20,46] in this way the observable o is evaluated by iteratively solving the two linear systems of equations:

$$\begin{aligned} \mathbf{A}'\mathbf{x} &= \mathbf{g}^0 \\ \mathbf{A}'^{\mathrm{T}}\tilde{\mathbf{x}} &= \mathbf{v} \end{aligned} \tag{45}$$

Iterative approximations $\mathbf{x}^{(i)}$ and $\tilde{\mathbf{x}}^{(i)}$ of the i-order and the corresponding residuals

$$\begin{aligned} \mathbf{r}^{(i)} &= \mathbf{g}^0 - \mathbf{A}\mathbf{x}^{(i)} \\ \tilde{\mathbf{r}}^{(i)} &= \mathbf{v} - \mathbf{A}^{\mathrm{T}}\tilde{\mathbf{x}}^{(i)} \end{aligned} \tag{46}$$

are calculated, and the convergence of the procedure is checked according to the criterion:

$$\tilde{\mathbf{r}}^{(i)\mathrm{T}} \mathbf{r}^{(i)} / \mathbf{v}^{\mathrm{T}} \mathbf{g}^0 \leq \delta \tag{47}$$

where δ is a constant which in our case was taken equal to 10^{-6}. The advantage over standard methods involving inversion of the $\mathbf{A}'$ matrix is 2-fold: both memory and computing time requirements are reduced. Convergence is reached with a number of matrix/vector products $M \ll N^T \sim 1000$, as would be required for the full inversion. Introduction of the induction contribution has the effect of slightly slowing down the convergence, however M remains of the order of 10−20. The memory saving depends on the fact that the $\mathbf{A}'$ matrix does not need to be stored. For the $\mathbf{A}$ contribution this is done as explained in ref 20: only the diagonal elements of the matrix representation of the S and D operators, which are evaluated by integration, are stored, while their off-diagonal elements are calculated when required. Also the elements of the matrix $\mathbf{A}^{\mathrm{ind}}$ can be recalculated at each time, provided that the matrix products appearing in eq 27 are efficiently implemented and the matrix $\mathbf{M}^{-1}$ is available.

Even though a very efficient way of solving the algebraic problem has been found, calculation of the term $U_{\mathrm{rf}}(\omega)$ remains computationally heavy, because of the need of exploring the space of the angular variables (θ, ϕ) specifying the molecular orientation. The integrals eq 37 are evaluated with the Gauss method, with Legendre and Chebyshev polynomials for the variables $t = cos(\theta)$ and $u = cos(\phi)$, respectively.[47] In our calculations 6 points in the range [0:1] were taken for the former variable and 24 points in correspondence of the range $[0:2\pi]$ for ϕ the angle, hence a total of 72 points to cover the whole angular space. Calculations were performed on a PENTIUM III-500 MHz PC; typically, calculation of each energy value eq 29 takes about 5 min; thus the complete evaluation of the reaction field contribution requires about 6 h. If compared with the same calculations performed in the absence of polarizability the computation time increases by less than 10%.

A fundamental ingredient required for the calculation of both the surface tensor and the reaction field contribution to the orienting potential is the molecular surface. This is defined according to the rolling sphere algorithm;[43,48] the implementation by Sanner[49] has been used. For a given molecule, the same surface is used for the surface tensor and the reaction field calculations; the number of tesserae N^T is obtained as a compromise between the requirements of limiting the dimension of the algebraic problem eq 42 and the need of obtaining accurate values of the reaction field energies $U_{\mathrm{rf}}(\omega)$, eq 29, as explained in ref 20.

Molecular geometries were determined by optimizing at the HF/6-31G* level with the analytical gradient procedure available in the GAUSSIAN 98 package.[50] Atomic charges were obtained by applying the Merz−Singh−Kollman scheme,[51] available in the same package, to the HF/6-31G* electrostatic potential.

V. Results and Discussion

Calculations were carried out for the aromatic molecules shown in Figure 1; the same molecules were considered in ref 20, where the results obtained in the absence of induction effects

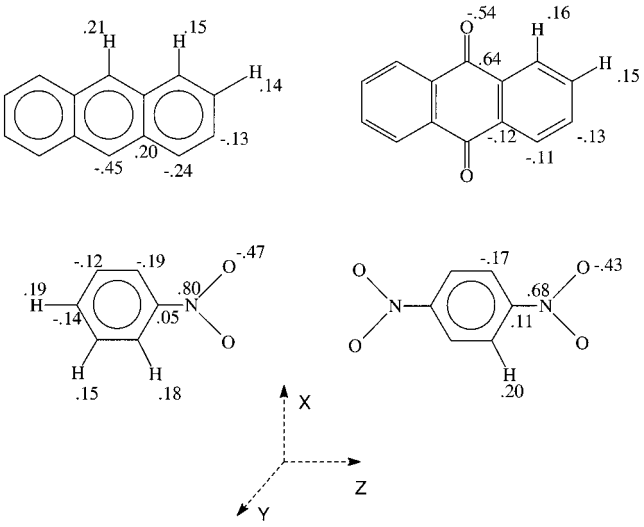

Figure 1. Chemical structure of the solutes under examination, with the atomic charges (au) calculated at the HF/6-31G* level.

TABLE 1: Principal and Average Values of the Molecular Polarizabilities (Å^3)[a]

		α_{xx}	α_{yy}	α_{zz}	$\bar{\alpha}$
anthracene	calc (a)	18.8	10.3	24.1	17.7
	calc (b)	23.3	23.3	23.3	23.3
	calc (c)	24.8	14.4	39.6	26.3
	exp[53]	22.4		39.0	
	exp[54]	25.6	15.2	35.2	25.6
	exp[55]				25.9
anthraquinone	calc (a)	20.0	10.7	25.0	
	exp[58]				24.5
nitrobenzene	calc (a)	11.0	6.4	12.5	10.0
	exp[56]	15.8	9.2	21.1	15.4
	exp[37]				12.9
p-dinitrobenzene	calc (a)	12.9	7.6	16.1	12.2
	exp[57]				18.4

[a] The theoretical values have been calculated with the Thole model (a), the additive approximation (b), and the Applequist method (c).

were reported and discussed. These are typical solutes used to probe ordering in liquid crystals, e.g., by NMR, with the advantageous feature of having simple nonflexible structures, similar shapes and quite different charge distributions: there is a nonpolar system, together with a molecule characterized by a strong dipole and two other nonpolar compounds, which, however, possess strong antiparallel dipoles.

The atomic charges, obtained with the Merz−Kollman−Singh scheme,[51] are also reported in Figure 1. For the definition of the molecular surface standard van der Waals radii were used[52] (r_C = 1.85 Å, r_N = 1.5 Å, r_O = 1.5 Å, $r_{H(ar)}$ = 1 Å) with a rolling sphere radius R = 3 Å and a vertex density of 5 Å^2.[49] This gives a number of tesserae of the order of 2000 for the molecules under investigation. For the molecular polarizability the van Duijnen parametrization of the Thole model has been used,[37] with the following values: α_C = 1.508 Å^3, α_N = 1.126 Å^3, α_O = 0.947 Å^3, α_H = 0.519 Å^3, and x = 1.7278 (see eq 20). Table 1 reports principal components and average value of the molecular polarizability tensors obtained in this way. In all cases the polarizability, which results to be anisotropic as a consequence of the spatial arrangement of the interacting dipoles, appears to be underestimated, both in its average value and in its anisotropy. As already mentioned in section II, this is not surprising in view of the model adopted for the polarizability. The parameters we have used were obtained by fitting experimental and ab initio molecular polarizabilities for a set of molecules including also a number of olefins and aromatic systems,[37] but for the latter the quality of the fits resulted to be inferior than in the case of aliphatic compounds; in particular, both average values and anisotropies of the polarizabilities appeared to be underestimated.

In our case, the quality of the predicted molecular polarizability can only be taken as an indication of the performance of the model used to describe it, but it cannot be the unique criterion to judge its suitability to be included in the reaction field treatment. Namely, the molecular polarizability accounts for the response of the electronic cloud to uniform electric fields, while the reaction field strongly depends on the position in the molecule. It is worth noting that in the isotropic phase the reaction field has the same symmetry of the molecule; therefore, it cannot induce perpendicular dipoles in aromatic molecules, as long as only point dipoles in the molecular plane are considered. Then, the response of the electronic charge distribution is independent of the perpendicular component of the polarizability. This is true even in the nematic phase, when the molecule has one of its principal axes parallel to the mesophase director; for intermediate orientations there will be some dependence, but strong effects are not physically reasonable. So, the isotropy of the atomic contributions, which might appear a major drawback of the Thole model when treating aromatic molecules, and really is in the case of the response to an applied uniform field breaking the symmetry, has no effects when the reaction field is considered. As far as anisotropic effects are concerned, the crucial aspect is the way of modeling the deformation of the electron cloud in the molecular plane. A closer insight into the induction effects in our systems can be gained by considering the atomic dipoles induced by the reaction field, calculated according to eq 30. Figures 2 and 3 show the dipole moments calculated for the molecules under investigation dissolved in an isotropic dielectric with permittivity ϵ = 10.17. The signs near the molecular surfaces correspond to the signs of the apparent charge density σ. The dipole distribution appears very reasonable, with dipoles directed according to the polarization of the nearby solvent and larger values on the atoms most exposed to the solvent. As a consequence of the molecular symmetry, no net dipole is induced in the molecules, with the exception of nitrobenzene. In this case an overall induced dipole of 1.79 D is predicted, with an increase of 35% with respect to the value calculated for the isolated molecule, which is 5.09 D.[20] Such an increase is comparable with the value of 44%, estimated for pure nitrobenzene from the refractive index and the dielectric constant in the liquid and in the gas phase; comparable increments were predicted for other polar molecules.[9,11]

For the sake of comparison, we shall also report the results obtained for anthracene using two alternative polarizability models. This molecule was chosen because for it all the required parameters are available in the literature. On one extreme, the simple additive approximation with noninteracting atomic dipoles has been considered; although this model, lacking any anisotropy, cannot provide a realistic estimate of the polarizability tensor, it can be useful for comparative purposes. On the opposite side, we have used the Applequist model of interacting monopoles−dipoles (see Appendix), which was devised just for aromatic molecules, and so we expect that a better account of the experimental behavior should be obtained.[30,32] In the first case the values proposed by Scheraga and co-workers,[34] α_C = 1.450 Å^3, α_H = 0.298 Å^3, were used. In the second the parametrization presented by Applequist was used with the so-called PNRI approximation[32] (partial neglect of ring interactions, i.e., the vertical dipoles at the carbon

position in the aromatic ring are decoupled from the other induced charges and dipoles), with $\tau_C = 0.228$, $\tau_H = 0$, $\alpha_H = 0.232$ Å^3, while anisotropic atomic polarizabilities were assumed for the aromatic carbons: $\alpha_{C\parallel} = 1.020$ Å^3, $\alpha_{C\perp} = 0.586$ Å^3. The principal polarizability values obtained with the two models are also reported in Table 1. Of course in the case of noninteracting isotropic atomic dipoles also the whole molecular polarizability comes out to be isotropic; however, the calculated value is not very far from the experimental average, reported in Table 1. On the contrary, good estimates of all the principal values of the polarizability tensor are provided by the Applequist model. So, from this point of view the latter seems to be more promising than the approach proposed by Thole. However, it should not be taken for granted that the features at the origin of the good performances of the Applequist model are really important for the description of the response to the nonuniform reaction field. First of all, the presence of anisotropic atom polarizabilities, which is important in determining the difference between the in-plane and out-of-plane components of the molecular polarizability, is irrelevant in the response of the charge distribution to the reaction field, as noted above. On the contrary, the description of the electronic deformation in the molecular plane, which is at the origin of the good prediction of the polarizability anisotropy in the molecular plane, is expected to have significant effects. Again, it is useful to look at the atom dipoles calculated with the different models. In the additive case the dipoles do not feel each other, so they simply reflect the polarizability values and the distance from the charged surface. The overall dipole distribution looks fairly similar to that obtained with the Thole model, with the main difference that in the absence of mutual interactions larger dipoles appear at the carbon positions. On the contrary, a quite peculiar dipole distribution, with a strong dependence of the magnitude on the atom position, is predicted by the Applequist approach. For the sake of comparison, the electronic deformation produced in anthracene by interactions with the solvent has also been estimated with ab initio methods. The atomic charges calculated in a vacuum (see Figure 1) have been compared with those obtained in the presence of a solvent with dielectric constant $\epsilon = 10.17$. The solvent effect was evaluated with the polarizable continuum model (PCM) for a self-consistent solution of the quantum mechanical problem of a molecule in a continuum dielectric, with a cavity defined by the united atom topological model, according to the standard procedure implemented in the package Gaussian 98.[50] Atomic charges were calculated in the same way as those in a vacuum, i.e., by applying the Merz−Singh−Kollman scheme[51] to the HF 6-31G* electrostatic potential. Comparable charge variations at all atomic positions have been obtained, of the order of ±0.1 au, in contrast with the predictions of the Applequist model. On the contrary, the quantum-mechanical picture resulted to be in qualitative agreement with that derived from the Thole model. The Applequist model differs from the Thole one for the absence of damping and the inclusion of induced charges; our calculations have shown that for anthracene the latter have only small effects, and the pronounced position dependence of the dipoles can be interpreted as an artifact deriving from the too strong couplings between nearby dipoles. So, we can conclude that the Thole model, although limited to a simple parametrization, which is not the optimal one for aromatic molecules and therefore cannot be expected to provide accurate estimates of the molecular polarizabilities, seems to be able to contain the relevant physical ingredient to give a reasonable picture of the response of the electron cloud to the nonuniform reaction field.

TABLE 2: Reaction Field Contribution to the Mean Field U^i_{rf}, $i \in \{x, y, z\}$, Calculated for a Solvent with Average Dielectric Permittivity $\bar{\epsilon}$ and Dielectric Anisotropy $\Delta\epsilon$, for the Molecular Orientation $i//\hat{n}$[a]

	$\bar{\epsilon} = 10.17$ $\Delta\epsilon = 0$	$\bar{\epsilon} = 10.17$ $\Delta\epsilon = 11.5$		
	U^0_{rf}	ΔU^x_{rf}	ΔU^y_{rf}	ΔU^z_{rf}
anthracene	−38727	1004	192	2448
b	−39823	1082	7	2829
c	−38278	1105	190	2283
anthraquinone	(−28947)	(527)	(25)	(1480)
nitrobenzene	−63786	2080	1463	752
p-dinitrobenzene	(−50063)	(1253)	(832)	(514)
	−49658	1588	1003	877
	(−38995)	(1024)	(564)	(552)
	−69847	2340	1421	710
	(−56677)	(1588)	(919)	(501)

[a] The difference $\Delta U^i_{rf} = U^i_{rf} - U_{rf,0}$ is calculated with respect to the value $U_{rf,0}$ corresponding to vanishing dielectric anisotropy. Energy is given in J mol^{-1}. Between brackets the values obtained by neglecting polarizability are reported (some of the values for *p*-dinitronitrobenzene are slightly different from those appearing in Table 2 of ref 20, where a misprint has been detected). Calculations have been performed with the Thole model for the polarizability, unless explicitly stated. [b] Additive approximation. [c] Applequist method.

The effects of polarizability on the reaction field energy U_{rf}, eq 29, can be seen in Table 2, which reports the values calculated for the molecules dissolved in solvents with vanishing dielectric anisotropy and dielectric constant $\epsilon = 10.17$. It appears from the table that in all cases the reaction field energies increase by more than 25% owing to the induction interactions. The magnitude of the effect increases with the dielectric constant and depends on the molecule; however, it is interesting to see that no simple correlation exists with the presence of strong dipoles, comparable changes being observed, e.g., for anthracene and nitrobenzene. In contrast with simple models, the absence of correlation between the reaction field and the presence of strong dipoles was also predicted when induction effects were neglected.[20] The increase of the solvent polarization can be easily understood in the case of a polarizable dipole enclosed in a spherical cavity in an isotropic dielectric: the permanent dipole $\vec{\mu}_0$ induces a polarization of opposite sign in the medium, which in turn induces an additional dipole parallel to $\vec{\mu}_0$ in the molecule.[22] For more complex cavity shapes and charge distributions, as occurs for real molecules, the effects are not so easy to be predicted, but it is reasonable to expect that in general the deformation of the electronic cloud will play in the direction of increasing the polarization of the surrounding dielectric.

Table 2 also displays the reaction field energies calculated for different orientations of the molecules in nematic solvents with positive dielectric anisotropy, expressed as differences with respect to the values obtained in solvents with the same average permittivity but vanishing dielectric anisotropy. We can see that also the orientation dependence of the reaction field energy becomes more pronounced when induction effects are taken into account, with a relative increase that generally is even larger than that in U^0_{rf}, the reaction field energy for $\Delta\epsilon = 0$. For anthracene we have also reported in Table 2 the results obtained by using the additive approximation (b) and the Applequist model for the polarizability (c). By comparing with the results of the Thole method we can see that, independently of the choice, alignment to the director of the perpendicular axis (*y*) is strongly favored, while in the molecular plane there is a strong propensity for the alignment of the short axis (*x*). In case (b) larger reaction field energies and energy differences are pre-

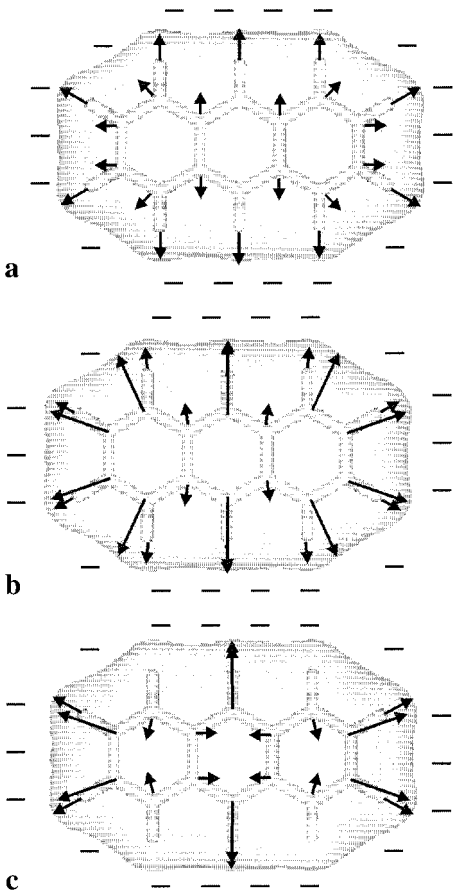

Figure 2. Dipole moments induced at the atomic positions by the reactions field ($\epsilon = 10.17$) for anthracene, calculated with the Thole model (a), the additive approximation (b), and the Applequist method (c). The signs near to the molecular surface indicate the solvent polarization. The length of the arrows is proportional to the magnitude of the induced dipole moments; for comparative purposes note that the dipole at the hydrogens linked to the C_9 and C_{10} atoms in (a) is 0.14 D. No arrow appears if the dipole moment is smaller than 0.05D.

dicted, in agreement with the presence of the fairly high induced dipoles, as seen before. On the contrary, in case (c) the results are not far from those obtained with the Thole polarizabilities, despite the differences in the induced dipole distribution discussed above. In all generality from the behavior of the anisotropies in the reaction field energy shown in Table 2 we can infer that, independently of the specific structure of the solute and the model used for the polarizability, inclusion of induction effects in the reaction field will increase the dependence of the solute order parameters on the dielectric anisotropy of the nematic solvent.

The changes in order parameters predicted when the molecules are dissolved in nematics with different permittivities are shown in Figures 4−7. Calculations have been performed with a mean field potential consisting of a reaction field and a surface tensor contribution, according to eq 32. The values of the surface tensor components for the molecules under examination can be found in ref 20. The ordering strength ξ is calculated from eq 41, by giving the axial component of the solvent surface tensor the value $T_s^{20} = 70$ Å^2, suitable for a typical nematogenic system like 4-pentyl-4′-cyanobiphenyl (5CB),[21] while reduced temperatures T/T^{NI} ranging between 0.77 and 1 have been considered. The results obtained for $\Delta\epsilon > 0$, $\Delta\epsilon < 0$, and $\Delta\epsilon = 0$ are shown in the figures. In the latter case the orientational order is fully determined by the short-range interactions, modeled by the surface tensor. For the case $\Delta\epsilon > 0$ we have

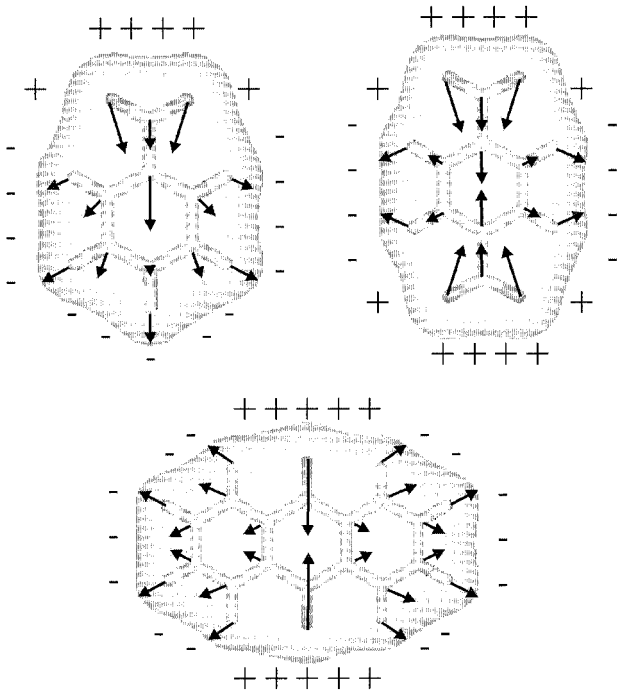

Figure 3. Dipole moments induced at the atomic positions by the reactions field for nitrobenzene, *p*-dinitrobenzene, and anthraquinone, as calculated with the Thole model. The signs near to the molecular surface indicate the solvent polarization. The length of the arrows is proportional to the magnitude of the induced dipole moments; in the case of anthraquinone induced dipoles are larger and a scale factor of $^1/_2$ is used. For comparative purposes note that the dipole at the hydrogens linked to the C_9 and C_{10} atoms in 2a is 0.14 D. No arrow appears if the dipole moment is smaller than 0.05 D.

assumed $T^{NI} = 308$ K, $\bar{\epsilon}^{NI} = 10.17$, $\Delta\epsilon^{NI} = 8$ (values appropriate for 5CB) while for $\Delta\epsilon < 0$ the values $T^{NI} = 320$ K, $\bar{\epsilon}^{NI} = 5.17$, $\Delta\epsilon^{NI} = -0.52$ have been taken, suitable for *N*-(4-methoxybenzylidene)-4-*n*-butylaniline (MBBA). Figures 4−7 display the biaxiality of order in the molecular plane, i.e., the difference $S_{zz} - S_{xx}$, as a function of the order parameter for the perpendicular axis, S_{yy}. Temperature is an implicit variable in such diagrams, since it decreases with increasing order. For $\Delta\epsilon > 0$ also the results obtained in the absence of induction interactions are shown in the figures (dashed line). It can be seen that introduction of the polarizability does not change the picture already drawn in ref 20, which can be summarized in the following way: electrostatic interactions have the effect of reducing the biaxiality of order in the molecular plane for anthracene, and they increase it for anthraquinone, nitrobenzene and *p*-dinitrobenzene. In all cases an increase of the magnitude of solvent effects by a factor of the order of 20−30% is observed, in comparison with calculations performed without polarizability. Only slight changes are predicted for $\Delta\epsilon < 0$ as a consequence of the small value of the dielectric anisotropy. For the sake of comparison, we show in Figures 4b and 5b experimental order parameters of anthracene and anthraquinone, for which data from NMR experiments in different solvents are available.[59−61] The reported data refer to the solvents PCH7 (4-cyano-(4′-*trans*-heptylcyclohexyl)benzene, $\bar{\epsilon}^{NI} \approx 7$, $\Delta\epsilon^{NI} \approx 8$), HAB (4,4′-di-*n*-heptylazoxybenzene, $\bar{\epsilon}^{NI} \approx 3.5$, $\Delta\epsilon^{NI} \approx 0.2$), Phase V (a commercial mixture of 4-*R*,4′-*R*′-azoxybenzene derivatives, each with a dielectric permittivity comparable with that of MBBA, so a small negative dielectric anisotropy is expected) and ZLI1167 (a commercial mixture of alkylcyanobicyclohexyls, which should then have a dielectric permittivity similar to that of PCH7). The correspondence between the

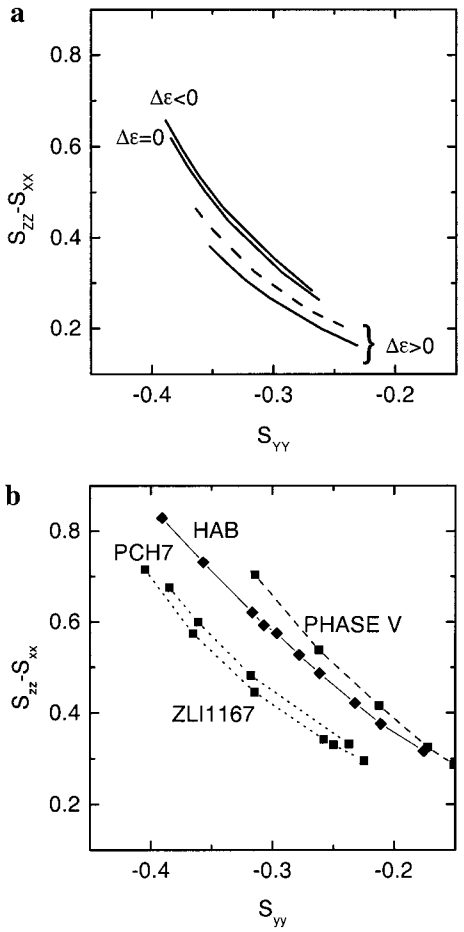

Figure 4. Orientational order parameters for anthracene in solvents with different dielectric anisotropies. (a) Calculated; the dashed lines indicate values obtained if induction effects are neglected. (b) Experimental data, from ref 59.

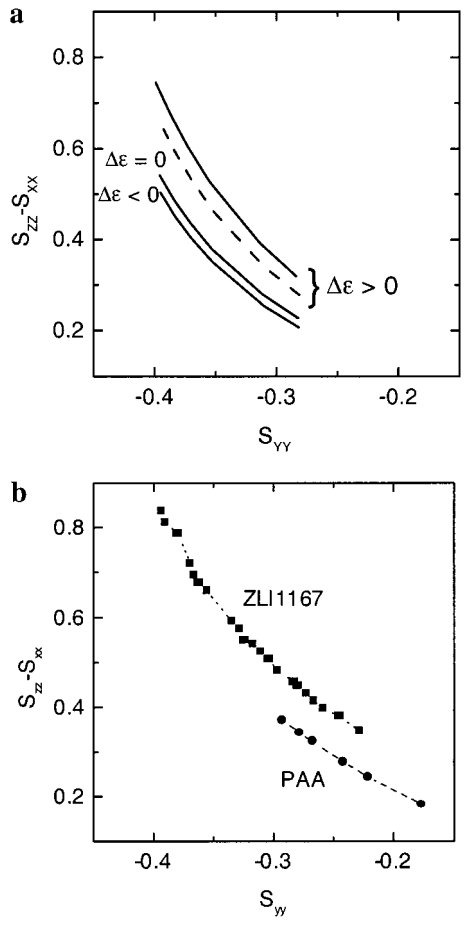

Figure 5. Order parameters for anthraquinone in solvents with different dielectric anisotropies: (a) calculated data, the dashed lines indicate values obtained if induction effects are neglected; (b) experimental data, from refs 60 for ZLI1167 and 61 for PAA.

predicted dependence on the dielectric anisotropy of the solvent and the measured changes of order clearly appears from the Figures 4a,b and 5a,b. According to both experiments and calculations the increase of the solvent dielectric anisotropy is accompanied by shifts in the biaxiality of order in opposite directions for anthracene and anthraquinone. So it occurs that, in contrast with what could be expected from the molecular shapes, the biaxiality of order in the ring plane is lower for anthracene than for anthraquinone, when dissolved in nematics with sufficiently high dielectric anisotropy. It can also be seen from the comparison of Figures 4a and 5a with Figures 4b and 5b that inclusion of the polarizability improves the agreement between computed and experimental results. The magnitude of such induction effects depends on how the polarizability is modeled. A comparison between the three variants considered in this work can be done for anthracene, on the basis of the anisotropy in the reaction field energy reported in Table 2. It comes out that similar effects on the orientational order are predicted with the Thole and the Applequist models, while larger changes would result if the additive approximation were used.

We can then conclude that the sizable increase of solvent effects on the orientational order of solutes resulting from the inclusion of polarizability in the reaction field goes in the direction of improving the agreement between theory and experiment. One reason for the discrepancies that still appear may reside in the approximate way of modeling polarizability. However, another and probably much more important reason can be devised in the crudeness of the method used for the short-range interactions. A more detailed approach, taking into account the molecular structure of the solvent is needed for a more accurate comparison between theory and experiments.[62]

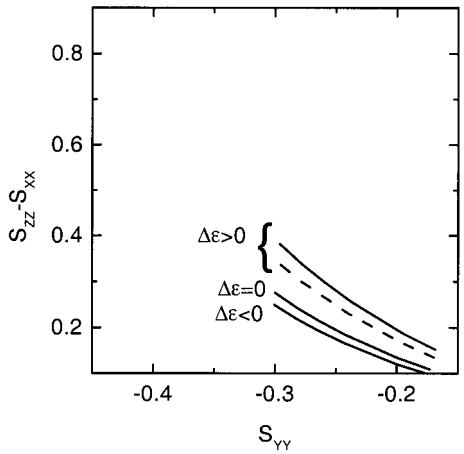

Figure 6. Predicted order parameters for nitrobenzene in solvents with different dielectric anisotropies (solid lines). The dashed lines indicate values obtained if induction effects are neglected.

VI. Conclusions

Here and in a previous paper[20] a reaction field method suitable for the evaluation of the electrostatic and induction contribution to the mean field potential experienced by molecules in liquid crystals has been set up. Such a work is motivated by the need

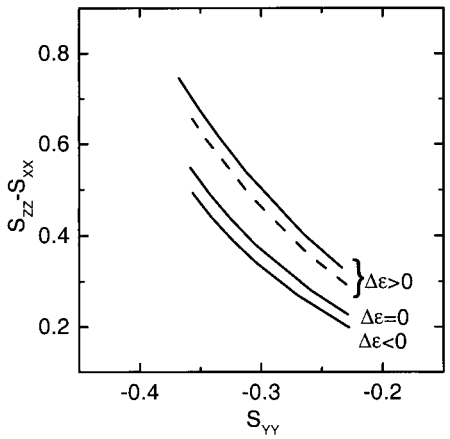

Figure 7. Predicted order parameters for *p*-dinitrobenzene in solvents with different dielectric anisotropies (solid lines). The dashed lines indicate the values obtained if induction effects are neglected.

of an approach going beyond simple toy models, but easier to handle than ab initio methods. So, while it should be able to give a realistic account of the main features of molecular structures, it is required to be sufficiently light to allow the calculation of the orientation dependence of the reaction field in anisotropic phases for molecules of a certain complexity, as the mesogenic systems are. In the present paper the previously developed reaction field treatment,[20] where the molecular charge distribution was assumed to be unaffected by the environment, has been extended to include induction interactions. This is important to complete our model, so that electrostatic effects on orientational order can be better estimated by assessing the role of the induction interactions. The work is also motivated by our intention of using this reaction field approach for the prediction of dielectric permittivity in liquid crystals, in what case polarizability is a relevant ingredient.[22]

At the semiphenomenological level that characterizes the treatment, the cavity shape is defined on the basis of the molecular structure and the permanent charge distribution is specified in terms of point charges located at the nuclear positions. In this context, induction effects are consistently included with a model of localized polarizabilities. The induction contribution can be easily embodied in the integral equation formalism used to solve the electrostatic problem, with a slight increase of the computational complexity. In the past, analogous methods for the calculation of the reaction field have been proposed, e.g., in the framework of electrostatic interactions in macromolecules.[9−12,41] The peculiarity of our approach derives from the fact that it is devised for the application to nematics; therefore (i) a suitable method for the solution of the electrostatic problem is used,[20,23] and (ii) the observables of interest depend on the anisotropy of induction interactions, which is not directly probed in the isotropic phase. The latter point implies that the choice of the model for the molecular polarizability may be more critical. We have used the Thole model of damped interacting dipoles located at the nuclear positions, which appears to provide a reasonable account of the local and overall response of a molecule to an applied electric field and for this reasons has also been used in other calculations of properties in condensed phases.[39−41] Such a model contains the essential ingredients in their simplest form; therefore it has the advantage of being of general use (a rather wide parametrization is available), although it may be not the optimal choice if a special class of molecules is considered. Anyway, our method is not restricted to a particular way of modeling distributed polarizabilities; alternative approaches have also been tried, and some results are reported in the paper.

Calculations performed on a set of test solutes have shown an increase by more than 20% in the reaction field energy by virtue of induction interactions in solvents with dielectric constant ϵ in the range between 5 and 10, with comparable effects for polar and nonpolar systems. Even larger increases are predicted for the anisotropy of the reaction field when the molecules are dissolved in solvents with nonzero dielectric anisotropy. Correspondingly, an enhancement of solvent effects on the orientational order parameters is observed, in comparison with what is predicted in the absence of polarizability, so improving the agreement with the experimental findings.

Acknowledgment. This work has been supported by MURST PRIN ex 40%, EC (TMR contract FMRX CT97 0121) and CNR, through its Centro Studi sugli Stati Molecolari. The authors gratefully acknowledge Prof. G.J. Moro for stimulating discussions.

Appendix

Interacting Monopoles−Dipoles.[30,32] According to this model each atom has a dipole polarizability α_J associated with an induced dipole according to eq 11, and a monopole polarizability τ_J related to the charge q_J^{ind} induced by the local potential, in our case the potential φ_J^{R} associated with the reaction field, by the expression

$$q_J^{\mathrm{ind}} = -\tau_J \varphi_J^{\mathrm{R}} \tag{A1}$$

Local field and potential at the *J*th atom position are determined by the reaction field and the induced charges and dipoles of all other atoms. Thus, in the case of a molecule with *N* atoms eq 14 can be generalized as

$$\mathbf{M}\mathbf{m}^{\mathrm{ind}} = \mathbf{e} \tag{A2}$$

where the column supermatrices $\mathbf{m}^{\mathrm{ind}}$ and $\mathbf{e}$ are defined as

$$\mathbf{m}^{\mathrm{ind}} = \begin{bmatrix} q_1^{\mathrm{ind}} \\ \vdots \\ q_n^{\mathrm{ind}} \\ \vec{\mu}_1^{\mathrm{ind}} \\ \vdots \\ \vec{\mu}_N^{\mathrm{ind}} \end{bmatrix} \qquad \boldsymbol{e} = \begin{bmatrix} -\varphi_1^R \\ \vdots \\ -\varphi_N^R \\ \vec{R}_1 \\ \vdots \\ \vec{R}_N \end{bmatrix} \tag{A3}$$

and $\mathbf{M}$ is a $4N \times 4N$ supermatrix given by

$$\boldsymbol{M} = \begin{bmatrix} \boldsymbol{M}^{00} & \boldsymbol{M}^{01} \\ \boldsymbol{M}^{10} & \boldsymbol{M}^{11} \end{bmatrix} \tag{A4}$$

where the matrix $\mathbf{M}^{11}$, of dimension $3N \times 3N$, coincides with the dipole supermatrix defined in eq 15, while the blocks $\mathbf{M}^{00}$, of dimension $N \times N$, and $\mathbf{M}^{01}$, $\mathbf{M}^{10}$, of dimension $N \times 3N$ and $3N \times N$, respectively, are given by

$$\mathbf{M}^{00} = \begin{bmatrix} \tau_1^{-1} & r_{12}^{-1} & \dots & r_{1N}^{-1} \\ r_{21}^{-1} & \tau_2^{-1} & \dots & r_{2N}^{-1} \\ \vdots & \vdots & & \vdots \\ r_{N1}^{-1} & r_{N2}^{-1} & \dots & \tau_N^{-1} \end{bmatrix}$$

$$-\mathbf{M}^{01} = (\mathbf{M}^{10})^{\mathrm{T}} = \begin{bmatrix} \vec{0} & \vec{t}_{12} & \dots & \vec{t}_{1N} \\ \vec{t}_{21} & \vec{0} & \dots & \vec{t}_{2N} \\ \vdots & \vdots & & \vdots \\ \vec{t}_{N1} & \vec{t}_{N2} & \dots & \vec{0} \end{bmatrix} \quad \text{(A5)}$$

with $\vec{t}_{IJ} = \vec{t}_I(\vec{r}_J)$.

Introduction of the electroneutrality constraint leads to the following expression for the relay matrix:[32]

$$[\mathbf{M}']^{pq}_{J\eta I\zeta} = [\mathbf{M}^{-1}] - \frac{\sum_{J'}[\mathbf{M}']^{p0}_{J\eta J'} \sum_{I'}[\mathbf{M}^{-1}]^{0q}_{I'I\zeta}}{\sum_{J'I'}[\mathbf{M}^{-1}]^{00}_{J'I'}} \quad \text{(A6)}$$

with

$$\eta, \zeta \in \{x, y, z\} \qquad \text{and} \qquad p, q \in \{0,1\}$$

Then, the Cartesian components of the molecular polarizability tensor can be calculated as

$$\alpha^{\mathrm{mol}}_{\eta\zeta} = \sum_{I=1}^{N}\sum_{J=1}^{N}\{r_J[\mathbf{M}']^{00}_{JI}r_{I\zeta} + [\mathbf{M}']^{10}_{J\eta I}r_{I\zeta} + r_{J\eta}[\mathbf{M}']^{01}_{JI\zeta} + [\mathbf{M}']^{11}_{J\eta I\zeta}\} \quad \text{(A7)}$$

The contribution of induced charges and dipoles to the electrostatic potential and field in $\vec{r}$ is given by (cfr eq 21).

$$\varphi^{\mathrm{ind}}(\vec{r}) = \sum_{J=1}^{N}\vec{t}_J(\vec{r})\cdot\vec{\mu}_J^{\mathrm{ind}} + \sum_{J=1}^{N}\frac{q_J^{\mathrm{ind}}}{4\pi\epsilon_0|\vec{r} - \vec{r}_J|}$$

$$\vec{E}^{\mathrm{ind}}(\vec{r}) = -\sum_{J=1}^{N}\boldsymbol{T}_J(\vec{r})\cdot\vec{\mu}_J^{\mathrm{ind}} + \sum_{J=1}^{N}\vec{t}_J(\vec{r})q_J^{\mathrm{ind}} \quad \text{(A8)}$$

Dipoles and charges induced by the reaction field can be obtained by substituting into eq A2 the expression for the reaction field at the nuclear positions, eq 23, and the corresponding potential:

$$\varphi_I^R = \frac{1}{4\pi\epsilon_0}\int_S \frac{1}{|\vec{r}_I - \vec{r}|}\sigma(\vec{r})\,\mathrm{d}\vec{r} \quad \text{(A9)}$$

so that

$$q_J^{\mathrm{ind}} = -\sum_I\left\{[\mathbf{M}']^{01}_{JI}\cdot\int_S\vec{t}_I(\vec{r})\,\sigma(\vec{r})\,\mathrm{d}\vec{r} + [\mathbf{M}']^{00}_{JI}\frac{1}{4\pi\epsilon_0}\int_S\frac{1}{|\vec{r}_I - \vec{r}|}\sigma(\vec{r})\,\mathrm{d}\vec{r}\right\}$$

$$\vec{\mu}_J^{\mathrm{ind}} = -\sum_I\left\{[\mathbf{M}']^{11}_{JI}\cdot\int_S\vec{t}_I(\vec{r})\,\sigma(\vec{r})\,\mathrm{d}\vec{r} + [\mathbf{M}']^{10}_{JI}\frac{1}{4\pi\epsilon_0}\int_S\frac{1}{|\vec{r}_I - \vec{r}|}\sigma(\vec{r})\,\mathrm{d}\vec{r}\right\} \quad \text{(A10)}$$

Finally, by using these expressions in eqs A8 we can write

$$\varphi^{\mathrm{ind}}(\vec{r}) = -\sum_{I,J}\left\{\left[\frac{1}{4\pi\epsilon_0|\vec{r} - \vec{r}_J|}[\mathbf{M}']^{00}_{JI} + \vec{t}_J(\vec{r})\cdot[\mathbf{M}']^{10}_{JI}\right]\times \frac{1}{4\pi\epsilon_0}\int_S\frac{1}{|\vec{r}_I - \vec{r}'|}\sigma(\vec{r}')\,\mathrm{d}\vec{r}' + \left[\frac{1}{4\pi\epsilon_0|\vec{r} - \vec{r}_J|}[\mathbf{M}']^{01}_{JI} + \vec{t}_J(\vec{r})\cdot[\mathbf{M}']^{11}_{JI}\right]\cdot\frac{1}{4\pi\epsilon_0}\int_S\vec{t}_I(\vec{r}')\,\sigma(\vec{r}')\,\mathrm{d}\vec{r}'\right\}$$

$$\vec{E}^{\mathrm{ind}}(\vec{r}) = \sum_{I,J}\left\{[-\vec{t}_J(\vec{r})[\mathbf{M}']^{00}_{JI} + \boldsymbol{T}_J(\vec{r})\cdot[\mathbf{M}']^{10}_{JI}]\times \frac{1}{4\pi\epsilon_0}\int_S\frac{1}{|\vec{r}_I - \vec{r}'|}\sigma(\vec{r}')\,\mathrm{d}\vec{r}' + [-\vec{t}_J(\vec{r})[\mathbf{M}']^{01}_{JI} + \mathbf{T}_J(\vec{r})\cdot[\mathbf{M}']^{11}_{JI}]\cdot\frac{1}{4\pi\epsilon_0}\int_S\vec{t}_I(\vec{r}')\,\sigma(\vec{r}')\,\mathrm{d}\vec{r}'\right\} \quad \text{(A11)}$$

If only polarizable dipoles are assumed, eqs 24 are recovered, where only the terms containing the diagonal block $[\mathbf{M}']^{11}$ of the relay matrix appear.

References and Notes

(1) Tomasi, J.; Persico, M. *Chem. Rev.* **1994**, *94*, 2027.
(2) Cramer, J. C.; Truhlar, D. G. *Chem. Rev.* **1999**, *99*, 2161.
(3) Amovilli, C.; Barone, V.; Cammi, R.; Cancès, E.; Cossi, M.; Mennucci, B.; Pomelli, C. S. *Adv. Quantum Chem.* **1998**, *32*, 227.
(4) Allen, M. P.; Tildesley, D. J. *Computer Simulations of Liquids*; Oxford University Press: Oxford, U.K., 1987.
(5) Davis, M. E.; McCammon, J. A. *Chem. Rev.* **1990,** *90*, 509.
(6) Hünenberger, P. H.; van Gunsteren, W. F. *J. Chem. Phys.* **1998**, *108*, 6117, and references therein.
(7) Liu, Y.-P.; Kim, K.; Berne, B. J.; Friesner, R. A.; Rick, S. W. *J. Chem Phys.* **1999**, *110*, 4739.
(8) Car, R.; Parrinello, M. *Phys. Rev. Lett.* **1985**, *55*, 2471.
(9) Sharp, K. A.; Honig, B. *Annu. Rev. Biophys. Biophys. Chem.* **1990**, *19*, 301.
(10) Sharp, K.; Jean-Charles, A.; Honig, B. *J. Phys. Chem.* **1992**, *96*, 3822.
(11) Rashin, A. *J. Phys. Chem.* **1990**, *94*, 1725.
(12) Warshel, A.; Levitt, M. *J. Mol. Biol.* **1976**, *103*, 227. Warshel, A.; Russel, S. T. *Proc. Nat. Acad. Sci., USA*, **1984**, *81*, 4785.
(13) Richardi, J.; Fries, P. H.; Krienke, H. *Mol. Phys.* **1999**, *96*, 1411.
(14) Vertogen, G.; de Jeu, W. H. *The Physics of Liquid Crystals, Fundamentals*; Springer: Berlin, 1988.
(15) Burnell, E. E.; de Lange, C. A. *Chem. Rev.* **1998**, *98*, 2539.
(16) Lemieux, R. P.; Williams, V. E. *J. Am. Chem. Soc.* **1998**, *120*, 11311.
(17) Berardi, R.; Orlandi, S.; Zannoni, C. *Chem. Phys. Lett.* **1996**, *261*, 357.
(18) McGrother, S.; Gil-Villegas, A.; Jackson, G. *Mol. Phys.* **1998**, *95*, 657.
(19) Terzis, A. F.; Photinos, D. J. *Mol. Phys.* **1994**, *83*, 847.
(20) di Matteo, A.; Ferrarini, A.; Moro, G. J. *J. Phys. Chem. B* **2000**, *104*, 7764.
(21) Ferrarini, A.; Moro, G. J.; Nordio, P. L.; Luckhurst, G. R. *Mol. Phys.* **1992**, *77*, 1.
(22) Böttcher, C. J. F.; Bordewijk, P. *Theory of Electric Polarization*; Elsevier: Amsterdam, 1973.
(23) Cancès, E.; Mennucci, B. *J. Math. Chem.* **1998**, *23*, 309.
(24) Banks, J. L.; Kaminski, G. A.; Zhou, R. H.; Mainz, D. T.; Berne, B. J.; Friesner, R. A. *J. Chem. Phys.* **2000**, *110*, 741.
(25) Chelli, R.; Ciabatti, S.; Cardini, G.; Righini, R.; Procacci, P. *J. Chem. Phys.* **1999**, *111*, 4218.
(26) Stone, A. J. *Mol. Phys.* **1985**, *56*, 1065.
(27) Le Sueur, R.; Stone, A. J. *Mol. Phys.* **1993**, *78*, 1267. Le Sueur, R.; Stone, A. J. *Mol. Phys.* **1994**, *83*, 293.
(28) Laidig, K. E.; Bader, R. F. W. *J. Chem. Phys.* **1990**, *93*, 7213. Bader, R. F. W.; Keith, T. A.; Gough, K. M.; Laidig, K. E. *Mol. Phys.* **1992**, *75*, 1167.
(29) Silberstein, L. *Philos. Mag.* **1917**, *33*, 521.
(30) Olson, M. L.; Sundberg, K. R. *J. Chem. Phys.* **1978**, *69*, 5400.
(31) Applequist, J. *Acc. Chem. Res.* **1977**, *10*, 79. Applequist, J.; Carl, J. R.; Fung, K. K. *J. Am. Chem. Soc.* **1972**, *94*, 2952.

(32) Applequist, J. *J. Phys. Chem.* **1993**, *97*, 6016. Applequist, J. *J. Chem. Phys.* **1985**, *83*, 809.
(33) Thole, B. T. *Chem. Phys.* **1981**, *59*, 341.
(34) No, K. T.; Cho, K. H.; Jhon, M. S.; Scheraga, H. A. *J. Am. Chem. Soc.* **1993**, *115*, 2005.
(35) Mortier, W. J.; Ghosh, S. K.; Shankar, S. *J. Am. Chem. Soc.* **1986**, *108*, 4315.
(36) Rappé, A. K.; Goddard, W. A. *J. Phys. Chem.* **1991**, *95*, 3358.
(37) van Duijnen, P. Th.; Swart, M. *J. Phys. Chem. A* **1998**, *102*, 2399.
(38) Jensen, L.; Åstrand, P.-O.; Sylvester-Hvid, K. O.; Mikkelsen, K. V. *J. Phys. Chem. A* **2000**, *104*, 1563.
(39) Burnham, C. J.; Li, J.; Xantheas, S. S.; Leslie, M. *J. Chem. Phys.* **1999**, *110*, 4566.
(40) Bernardo, D. N.; Ding, Y.; Krogh-Jespersen, K.; Levy, R. M. *J. Phys. Chem.* **1994**, *98*, 4180.
(41) Rullmann, J. A. C.; Bellido, M. N.; van Duijnen, P. Th. *J. Mol. Biol.* **1989**, *206*, 101.
(42) Buckingam, A. D. *Adv. Chem. Phys.* **1967**, *12*, 107.
(43) Janssen, F.; Moro, G. J.; Nordio, P. L. *Liq. Cryst.* **1999**, *26*, 201.
(44) The parameter ξ is related to the parameter ϵ used in previous works by the relation $\xi = k_B T\epsilon$.
(45) Zare, N. R. *Angular Momentum*; Wiley: New York, 1987.
(46) Barrett, R.; Berry; M.; Chan, T. F.; Demmel; J.; Donato, J. M.; Dongarra, J.; Eijkhout, V.; Pozo, R.; Romine, C.; Van der Vorst, H. *Templates for the Solution of Linear Systems: Building Blocks for Iterative Methods*; SIAM: Philadelphia, 1994.
(47) Press, W. H.; Flannery, B. P.; Teukolsky, S. A.; Vetterling, W. T. *Numerical Recipes*; Cambridge University, Cambridge, 1988.
(48) Richards, F. M. *Annu. Rev. Biophys. Bioeng.* **1977**, *151*, 6. Connolly, M. L. *J. Appl. Crystallogr.* **1983**, *16*, 548.
(49) Sanner, M. F.; Spenher, J.-C.; Olson, A. J. *Biopolymers* **1996**, *38*, 305.
(50) Frisch, M. J.; Trucks, G. W.; Schlegel, H. B.; Scuseria, G. E.; Robb, M. A.; Cheeseman, J. R.; Zakrzewski, V. G.; Montgomery, J. A., Jr.; Stratmann, R. E.; Burant, J. C.; Dapprich, S.; Millam, J. M.; Daniels, A. D.; Kudin, K. N.; Strain, M. C.; Farkas, O.; Tomasi, J.; Barone, V.; Cossi, M.; Cammi, R.; Mennucci, B.; Pomelli, C.; Adamo C.; Clifford, S.; Ochterski, J.; Petersson, G. A.; Ayala, P. Y.; Cui, Q.; Morokuma, K.; Malick, D. K.; Rabuck, A. D.; Raghavachari, K.; Foresman, J. B.; Cioslowski, J.; Ortiz, J. V.; Baboul, A. G.; Stefanov, B. B.; Liu, G.; Liashenko, A.; Piskorz, P.; Komaromi, I.; Gomperts, R.; Martin, R. L.; Fox, D. J.; Keith, T.; Al-Laham, M. A.; Peng, C. Y.; Nanayakkara, A.; Gonzalez, C.; Challacombe, M.; Gill, P. M. W.; Johnson, B.; Chen, W.; Wong, M. W.; Andres, J. L.; Gonzalez, C.; Head-Gordon, M.; Replogle, E. S.; and Pople. J. A. *Gaussian 98*, Revision A.7; Gaussian Inc.: Pittsburgh, PA, 1998.
(51) Besler, B. H.; Merz, K. M.; Kollman, P. A. *J. Comput. Chem.* **1990**, *11*, 431. Singh, U. C.; Kollman, P. A. *J. Comput. Chem.* **1984**, *5*, 129.
(52) Bondi, A. *J. Phys. Chem.* **1964**, *68*, 441.
(53) Cheng, C. L.; Murthy, D. S. N.; Richtie, G. L. D. *Aust. J. Chem.* **1972**, *25*, 1301.
(54) Zamani-Khamiri, O.; Hameka, H. F. J. *J. Chem. Phys.* **1979**, *71*, 1607.
(55) Schuyer, J.; Blom, L.; van Krevelen, D. W. *Trans. Faraday Soc.* **1953**, *49*, 1391.
(56) Chelkowski, A. *Dielectric Physics*; Elsevier, Amsterdam, 1980.
(57) *Handbook Chemistry and Physics*; Weast, R. C., Ed.; CRC: Cleveland, OH, 1996.
(58) Schuyler, J.; Blom, L.; van Krevelen, D. W. *Trans. Faraday Soc.* **1953**, *49*, 1391.
(59) Emsley, J. W.; Hashim, R.; Luckhurst, G. R.; Shilstone, G. N. *Liq. Cryst.* **1986**, *5*, 437.
(60) Tarroni, R.; Zannoni, C. *J. Phys. Chem.* **1996**, *100*, 17157.
(61) Emsley, J. W.; Heeks, S. H.; Horne, T. J.; Howells, M. H.; Moon, A.; Palke, W. E.; Patel, S. U.; Shilstone, G. N.; Smith, A. *Liq. Cryst.* **1991**, *9*, 649.
(62) Ferrarini, A.; Moro, G. J. *J. Chem. Phys.* **2001**, *114*, 596.